Composite Centered Schemes for Multidimensional Conservation Laws

Richard Liska[1] and Burton Wendroff[2]

Abstract. The oscillations of a centered second order finite difference scheme and the excessive diffusion of a first order centered scheme can be overcome by global composition of the two, that is by performing cycles consisting of several time steps of the second order method followed by one step of the diffusive method. We show the effectiveness of this approach on some test problems in two and three dimensions.

1. Introduction

For a system of conservation laws $U_t = f_x(U)$, it is well known that the Lax-Wendroff (LW) finite difference scheme produces oscillations behind shock waves while the Lax-Friedrichs (LF) method is excessively diffusive, smearing out the shocks more than is usually acceptable. Simple two-step versions of both schemes are defined as follows. For both schemes the first half step defines new values on a staggered dual grid as

$$U_{i+1/2}^{n+1/2} = \frac{1}{2}[U_i^n + U_{i+1}^n] + \frac{\Delta t}{2\Delta x}[f(U_{i+1}^n) - f(U_i^n)]. \tag{1}$$

The second half step of the LF scheme is given by the same formula (1) shifted by $1/2$ in the index i and operates from the time level $n+1/2$ to the level $n+1$. The second half step of the LW scheme however corrects from the time level n to the time level $n+1$ using the fluxes from the time level $n+1/2$,

$$U_i^{n+1} = U_i^n + \frac{\Delta t}{\Delta x}[f(U_{i+1/2}^{n+1/2}) - f(U_{i-1/2}^{n+1/2})]. \tag{2}$$

To demonstrate the properties of these schemes we use the shallow water equations [1]

$$\begin{aligned} h_t + (hu)_x &= 0 \\ (hu)_t + \left(hu^2 + g\frac{1}{2}h^2\right)_x + ghz_{0x} &= 0, \end{aligned}$$

where $h(x,t)$ is the thickness of the water layer, $u(x,t)$ is the velocity of the layer, $z_0(x)$ is the height of the bottom and g is the gravitational constant. The bottom profile $z_0(x) = \max(0, b_c(1-x^2/4))$ is used here. The initial conditions are $h(x,0)+$

$z_0(x) = 1, u(x,0) = u_0$. The oscillations and excessive diffusion phenomena are evident in Fig. 1(a), where the height of the 1D shallow water flow over topography calculated by LF and LW schemes is presented for a problem on $x \in (-10, 10)$ with $b_c = 0.3, u_0 = 1, g = 1$, the solution is plotted at $t = 20$.

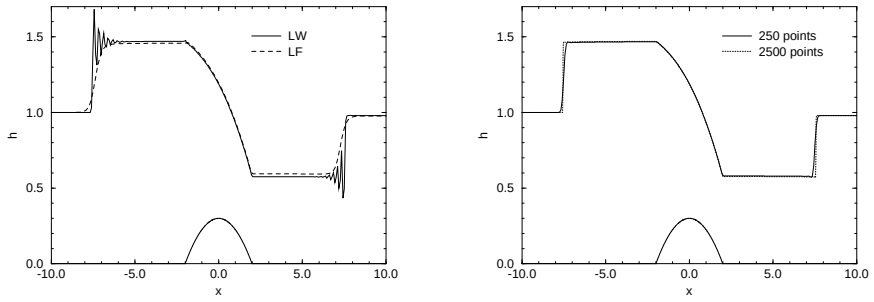

(a) (b)

FIGURE 1. Height of a 1D shallow water flow calculated by (a) LW and LF schemes with 250 points and (b) by composite LWLF4 scheme with 250 and 2500 points.

We have found an effective way to overcome this behavior of the two methods is to compose them. Thus, the composite scheme is defined by global composition of several LW steps followed by one LF step. If we denote by L_W the operator defined by the LW scheme (1),(2) and by L_F the operator defined by the LF scheme (1), then difference operator S_k defined by $k-1$ applications of L_W followed by one application of L_F

$$S_k = L_F \circ L_W \circ L_W \circ \cdots \circ L_W, \tag{3}$$

defines the composite scheme which we call LWLFk. The operator S_k operates from time level n to $n+k$, $U^{n+k} = S_k U^n$. The results of the same problem done by the composite LWLF4 scheme with 250 and 2500 points presented in Fig. 1(b) show that the composite scheme eliminates the drawbacks of both LW and LF schemes. The solution is not oscillatory and the shock heights and speeds are resolved well. The solution with 2500 points is presented as a good approximation of the exact solution.

The LW scheme is second order while LF is only first order accurate which implies that the composite scheme is also only first order, however with a smaller coefficient of the leading error term. For more details of composite schemes see [2]. Other 1D shallow water problems are treated by composite schemes in [3].

Our goal here is to show that this idea of composing schemes is also effective in higher dimensions. In [2] we developed a new version of Lax-Friedrichs in two dimensions that is used as a predictor for Lax-Wendroff. In the remainder of the

paper we review this method and present a modification necessary to use it in three dimensions. We then show the results of some two and three dimensional test problems.

Our aproach requires neither eigenvector decomposition nor Riemann solvers and thus the method is fast. Recently the interest in such decomposition-free and Riemann-solver-free methods has been renewed [4, 5, 6].

2. Treating 2D

The basic idea of the new version of 2D Lax-Friedrichs, which is derived in [2], is based on the observation of Boukadida and LeRoux [7] that in order to implement a two-dimensional Godunov method to get cell averages on the dual grid from the averages on the primary grid one need only solve one-dimensional Riemann problems on the edges of the dual grid. The first half step of the new LF is, for the system of 2D conservation laws $U_t = f_x(U) + g_y(U)$, given by

$$\begin{aligned} U^{n+1/2}_{i+1/2,j+1/2} &= \frac{1}{4}[U^n_{i,j} + U^n_{i+1,j} + U^n_{i,j+1} + U^n_{i+1,j+1}] \\ &\quad + \frac{\Delta t}{2\Delta x}[F_{i+1,j+1/2} - F_{i,j+1/2}] + \frac{\Delta t}{2\Delta y}[G_{i+1/2,j+1} - G_{i+1/2,j}], \end{aligned} \tag{4}$$

where the fluxes F, G are evaluated at the LF approximate solution of the 1D Riemann problems at time level $n + 1/4$, giving

$$\begin{aligned} F_{i+1,j+1/2} &= f\left(\frac{1}{2}[U^n_{i+1,j+1} + U^n_{i+1,j}] + \frac{\Delta t}{4\Delta y}[g(U^n_{i+1,j+1}) - g(U^n_{i+1,j})]\right), \\ G_{i+1/2,j+1} &= g\left(\frac{1}{2}[U^n_{i+1,j+1} + U^n_{i,j+1}] + \frac{\Delta t}{4\Delta x}[f(U^n_{i+1,j+1}) - f(U^n_{i,j+1})]\right). \end{aligned}$$

The second half step of the LF scheme going from the dual to the primary mesh is given by the same formulas shifted by $1/2$ in the indices i, j.

The corresponding second order accurate predictor-corrector scheme, which we call corrected Lax-Friedrichs (CF), is then

$$\begin{aligned} U^{n+1}_{i,j} &= U^n_{i,j} \\ &+ \frac{\Delta t}{2\Delta x}[f(U^{n+1/2}_{i+1/2,j+1/2}) + f(U^{n+1/2}_{i+1/2,j-1/2}) - f(U^{n+1/2}_{i-1/2,j+1/2}) - f(U^{n+1/2}_{i-1/2,j-1/2})] \\ &+ \frac{\Delta t}{2\Delta y}[g(U^{n+1/2}_{i+1/2,j+1/2}) + g(U^{n+1/2}_{i-1/2,j+1/2}) - g(U^{n+1/2}_{i+1/2,j-1/2}) - g(U^{n+1/2}_{i-1/2,j-1/2})] \end{aligned}$$

where the predictor half-step is defined by the LF half step (4).

The composite schemes are constructed by the same way as in 1D (3) and are denoted by CFLFk. For more details see [2] where we have shown that both the LF and CF schemes are optimally stable for the scalar advection equation with $f = aU, g = bU$, i.e. their stability condition is $\max(|a\Delta t/\Delta x|, |b\Delta t/\Delta x|) \leq 1$, which is also the stability condition of the composite schemes in that case. No stability analysis is available for systems, but our experience indicates that the

composite schemes are stable if $\max(|\alpha_i|\Delta t/\Delta x, |\beta_j|\Delta t/\Delta x) \leq 1$, where α_i and β_j are eigenvalues of x and y flux Jacobian matrices. The time interval Δt is adaptively determined from this stability condition after each time step.

The presented 2D LF, CF and composite schemes can be generalized also to trapezoidal meshes [8].

The composite schemes proved to work well on several 2D Euler gas dynamics tests [2] and on 2D shallow water equations [8]. Here we present the solution of two Riemann problems for 2D ideal gas Euler equations (2D analog of (9) with density ρ velocities u, v, total energy E and pressure p for gas with $\gamma = 1.4$) from [9, 10].

The problems are solved in the $x - y$ region $(0, 1) \times (0, 1)$. The region is divided by two lines $x = 1/2, y = 1/2$ into four quadrants. The initial data consists of a single constant state in each of the four quadrants. We will use the subscripts ll, lr, ul, ur to denote lower-left, lower-right, upper-left and upper-right quadrants respectively. These constant states are chosen so that each pair of quadrants defines a one-dimensional Riemann problem producing a single wave, which could be a shock, rarefaction or slip contact discontinuity. The first example is the configuration 3 from [10] with initial conditions for $V = (p, \rho, u, v)$ in the four quadrants $V_{ll} = (0.029, 0.138, 1.206, 1.206)$, $V_{lr} = (0.3, 0.5323, 0, 1.206)$, $V_{ul} = (0.3, 0.5323, 1.206, 0)$, $V_{ur} = (1.5, 1.5, 0, 0)$. For this configuration four backward moving shocks are produced. The contour map of density at $t = 0.3$ for this problem solved on 400×400 mesh by the CFLF8 scheme is presented in Fig. 2(a). The second example is the configuration 12 from [10] with initial conditions $V_{ll} = (1, 0.8, 0, 0)$, $V_{lr} = (1, 1, 0, 0.7276)$, $V_{ul} = (1, 1, 0.7276, 0)$, $V_{ur} = (0.4, 0.5313, 0, 0)$. For this configuration two forward moving shocks and two standing slip contact discontinuities are produced. The contour map of density at $t = 0.25$ for this problem solved on 400×400 mesh by the CFLF8 scheme is presented in Fig. 2(b).

The shocks and other structures are resolved well. There is an overshoot at the curved shocks in Fig. 2(b). Results are similar to those published in [9, 10].

In [2] we have also experimented with a second order diffusive WENO [11] scheme replacing the LF step in the composite schemes. We do not use the eigenvector decomposition as in [11] and apply the WENO procedure directly to the conserved variables.

3. Extending to 3D

In this section we develop and analyze the new LF and CF schemes in 3D for a 3D system of conservation laws $U_t = f_x(U) + g_y(U) + h_z(U)$. The schemes are again two-step with predictor and corrector and their construction is based on similar ideas as in 2D.

3.1. LF Scheme in 3D

The LF predictor working from the original to the dual grid is derived by integrating the 3D system over the whole 3D grid cell and over the time interval with

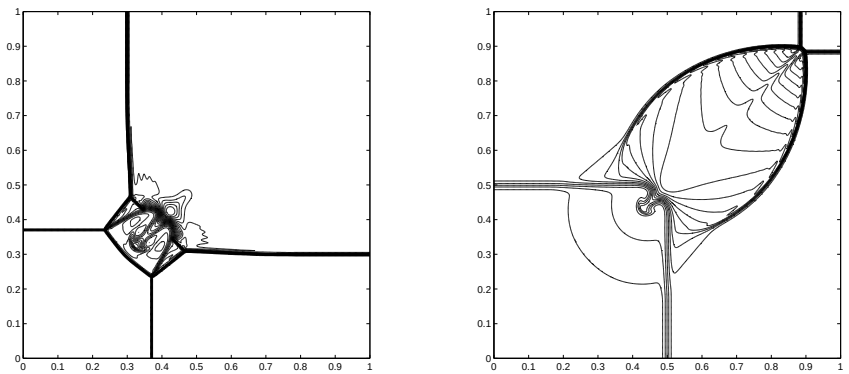

(a) (b)

FIGURE 2. Contour plot of density for configuration 3 (a) and configuration 12 (b).

length $\Delta t/2$. The integration gives

$$\begin{aligned} U^{n+1/2}_{i+1/2,j+1/2,k+1/2} &= \frac{1}{8}(U_{i,j,k}+U_{i+1,j,k}+U_{i,j+1,k}+U_{i,j,k+1} \\ &\quad +U_{i,j+1,k+1}+U_{i+1,j+1,k}+U_{i+1,j,k+1}+U_{i+1,j+1,k+1}) \\ &\quad +\frac{1}{2}\frac{\Delta t}{\Delta x}(F_{i+1,j+1/2,k+1/2}-F_{i,j+1/2,k+1/2}) \\ &\quad +\frac{1}{2}\frac{\Delta t}{\Delta y}(G_{i+1/2,j+1,k+1/2}-G_{i+1/2,j,k+1/2}) \\ &\quad +\frac{1}{2}\frac{\Delta t}{\Delta z}(H_{i+1/2,j+1/2,k+1}-H_{i+1/2,j+1/2,k}) \end{aligned} \tag{5}$$

with the fluxes at the center of faces given by the LF approximation of a corresponding 2D Riemann problem, that is,

$$\begin{aligned} F_{i,j+1/2,k+1/2} &= f\left[\frac{1}{4}(U_{i,j,k}+U_{i,j+1,k}+U_{i,j,k+1}+U_{i,j+1,k+1})\right. \\ &\quad +\frac{1}{4}\frac{\Delta t}{\Delta y}(g(U_{i,j+1,k+1/2})-g(U_{i,j,k+1/2})) \\ &\quad \left.+\frac{1}{4}\frac{\Delta t}{\Delta z}(h(U_{i,j+1/2,k+1})-h(U_{i,j+1/2,k}))\right] \end{aligned} \tag{6}$$

with similar expressions for G and H. The solution at the center of edges is given by the LF approximation of associated 1D Riemann problems

$$U_{i+1/2,j,k} = \frac{1}{2}(U_{i,j,k}+U_{i+1,j,k})+C\frac{\Delta t}{\Delta x}(f(U_{i+1,j,k})-f(U_{i,j,k}))$$

with similar formulas for $U_{i,j+1/2,k}$ and $U_{i,j,k+1/2}$. The LF corrector is the same as the predictor (5) with primary and dual grids exchanged.

With $C = 1/6$, for scalar advection the LF half step is the transport projection scheme with coefficients $(1 \pm \lambda)(1 \pm \mu)(1 \pm \tau)$, where λ, μ, τ are CFL numbers, i.e. for $f(u) = au$ is $\lambda = a\Delta t/\Delta x$ etc. For $\max(|\lambda|, |\mu|, |\tau|) \leq 1$ the LF half step is a positive scheme and so it is optimally stable.

3.2. CF Scheme in 3D

The CF predictor is again the same as the LF predictor (5), however, for stability reasons we will vary the constant C. The CF corrector is a standard centered correction from time level n to time level $n+1$ with fluxes on the staggered grid at time level $n + 1/2$,

$$\begin{aligned} U^{n+1}_{i,j,k} &= U^n_{i,j,k} + \frac{\Delta t}{\Delta x}(F_{i+1/2,j,k} - F_{i-1/2,j,k}) \\ &\quad + \frac{\Delta t}{\Delta y}(G_{i,j+1/2,k} - G_{i,j-1/2,k}) + \frac{\Delta t}{\Delta z}(H_{i,j,k+1/2} - H_{i,j,k-1/2}), \end{aligned} \tag{7}$$

where

$$\begin{aligned} F_{i+1/2,j,k} &= \frac{1}{4}[f(U^{n+1/2}_{i+1/2,j-1/2,k-1/2}) + f(U^{n+1/2}_{i+1/2,j+1/2,k-1/2}) \\ &\quad + f(U^{n+1/2}_{i+1/2,j-1/2,k+1/2}) + f(U^{n+1/2}_{i+1/2,j+1/2,k+1/2})], \end{aligned} \tag{8}$$

and similarly for G and H.

The composite schemes are again defined the same as in 1D and 2D by (3).

In [2] it was shown that for scalar advection with $C = 1/6$ in the predictor the CF scheme is unconditionaly unstable (composite schemes are suboptimally stable). The modified equation approach revealed that the instability is caused by terms $U_{xxyz}, U_{xyyz}, U_{xyzz}$ which come from flux terms of the form $f(g(h(u)))$ (with arbitrary ordered f, g, h), which leads us to variations of the constant C. The predictor with $C = 0$ has for scalar advection the coefficients $(1 \pm \lambda)(1 \pm \mu)(1 \pm \tau) \pm \lambda\mu\tau$, which do not include the term $\lambda\mu\tau$ which is related to stability. With $C = 0$ in the predictor the CF scheme is suboptimally stable with quite a big stability region including the cube $\max(|\lambda|, |\mu|, |\tau|) < 0.8545$. For the case $\lambda = \mu = \tau$ we have proved, by using the quantifier elimination approach [12], that the scheme is stable iff $27\lambda^8 - 18\lambda^4 + 4\lambda^2 - 1 \leq 0$.

3.3. Simpler Schemes

A simpler 3D LF scheme can be obtained by using the simple fluxes

$$\begin{aligned} F_{i,j+1/2,k+1/2} &= \frac{1}{4}[f(U_{i,j,k}) + f(U_{i,j+1,k}) + f(U_{i,j,k+1}) + f(U_{i,j+1,k+1})] \\ G_{i+1/2,j,k+1/2} &= \frac{1}{4}[g(U_{i,j,k}) + g(U_{i+1,j,k}) + g(U_{i,j,k+1}) + g(U_{i+1,j,k+1})] \\ H_{i+1/2,j+1/2,k} &= \frac{1}{4}[h(U_{i,j,k}) + h(U_{i,j+1,k}) + h(U_{i+1,j,k}) + h(U_{i+1,j+1,k})] \end{aligned}$$

in (5) instead of (6), as proposed in [13]. Of course, schemes using these fluxes are faster so we call the corresponding schemes fast LF (FLF) and fast CF (FCF).

Composites are again constructed as in (3). The FLF and FCF schemes are faster, but they have a more restrictive stability condition. For the case $\lambda = \mu = \tau$ both are stable for $|\lambda| < 1/\sqrt{3} \approx 0.577$. Their stability domain includes the box $(-1/\sqrt{3}, 1/\sqrt{3})^3$ in the λ, μ, τ space. Note, however, that using the adaptive time step based on the worst-case point of the computational domain we often can compute with a higher CFL limit as in section 4.2.

For our problems these simpler composite schemes worked very well producing results close to the CFLFn composites.

4. Numerical Results in 3D

We present here two 3D examples using Euler equations for an ideal gas

$$\begin{pmatrix} \rho \\ \rho u \\ \rho v \\ \rho w \\ E \end{pmatrix}_t + \begin{pmatrix} \rho u \\ \rho u^2 + p \\ \rho uv \\ \rho uw \\ u(E+p) \end{pmatrix}_x + \begin{pmatrix} \rho v \\ \rho uv \\ \rho v^2 + p \\ \rho vw \\ v(E+p) \end{pmatrix}_y + \begin{pmatrix} \rho w \\ \rho uw \\ \rho vw \\ \rho w^2 + p \\ w(E+p) \end{pmatrix}_z = 0 \qquad (9)$$

with density ρ velocity (u, v, w), energy E and pressure $p = (\gamma - 1)[E - 1/2\rho(u^2 + v^2 + w^2)]$.

4.1. Noh's Problem in 3D

The first example is the Noh's problem [14] for idea gas with $\gamma = 5/3$. The initial density is 1, velocity points to origin and has magnitude 1 and pressure is zero. The exact solution of this problem is a spherical shock moving with velocity $v = 1/3$ from the origin. The pre-shock values for $r > vt$ (r is distance from origin $r = \sqrt{x^2 + y^2 + z^2}$) are $\rho^- = (1 + t/r)^2$, $p^- = 0$, $|(u, v, w)^-|^2 = 1$ and points to origin. The post shock values for $r < vt$ are constants $\rho^+ = 64$, $(u, v, w)^+ = 0, p^+ = 64/3$.

In Fig. 3 we present numerical results of the Noh's problem at $t = 1$ solved in the cube $(0, 0.5)^3$ by the CFLF8 scheme with CFL limit 0.8 with symmetric boundary conditions on the inner faces $x = 0, y = 0, z = 0$ and exact boundary conditions on the outer faces $x = 0.5, y = 0.5, z = 0.5$ (we might use free boundary conditions on outer faces but then we would need either to compute on a larger domain or only up to a smaller time). The convergence to exact solution is shown on Fig. 3(a). Fig. 3(b) shows that the spherical symmetry of the numerical solution is well preserved.

4.2. Spherical Riemann Problem between Two Walls

This example comes from [15, 16]. An ideal gas with $\gamma = 1.4$ is located in the slab $0 < z < 1$ with two boundary walls at $z = 0$ and $z = 1$. The initial density is 1 everywhere, initial pressure is 5 inside the sphere centered at (0,0,0.4) with radius 0.2 and 1 outside the sphere and the gas is initially at rest. The initial data result in an outward moving shock and a contact discontinuity and an inward moving rarefaction wave which reflects from the sphere center as the second shock wave.

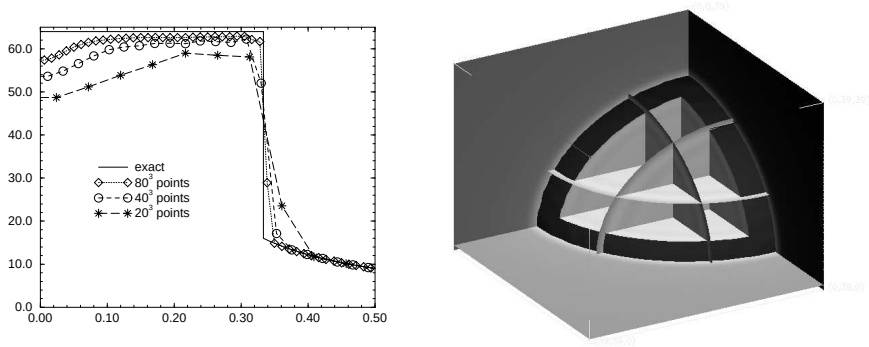

(a) (b)

FIGURE 3. Density of Noh's problem at $t = 1$ computed by CFLF8 scheme: (a) convergence test done on $20^3, 40^4, 80^3$ points compared with exact solution, plotted are values on the diagonal $x = y = z$, (b) 3D view of spherical symmetry solution using 40^3 cells

After reflecting from the walls quite a complex structure of waves is obtained. The problem is solved in the box $(x, y, z) \in (0, 1.5)^2 \times (0, 1)$ with reflecting boundary conditions at the walls, symmetric boundary conditions on the inner faces $x = 0, y = 0$ and free boundary conditions on the outer faces $x = 1.5, y = 1.5$. In Fig. 4 we present results of FCFFLF8 scheme on the mesh of $300 \times 300 \times 200$ points with CFL limit 0.8 at time $t = 0.7$. The contour plot of pressure at the $y = 0$ face is presented in Fig. 4(a) and a scatter plot of pressure versus the distance from the z axis at the plane $z = 0.4$ is presented in Fig. 4(b).

5. Concluding Remarks

The composite schemes are simple, require neither eigenvector decomposition nor Riemann solvers, and thus they are fast. They work well for a variety of problems, so it seems that they are also robust. Note also that they are ideally suited for parallelization and vectorization; actually, the computation on the large $300 \times 300 \times 200$ mesh presented in the section 4.2 has been done on a vector computer.

We have been also experimenting with using component-wise WENO [2, 11] scheme (CW) in the composites instead of the LF scheme. For Noh's problem we have obtained better convergence both in 2D and 3D, however for the 3D spherical Riemann problem the CFCW composites are unstable. For 2D Riemann problems the CFCW composites are noisier than CFLF composites [2].

As concerns speed, the CW scheme is about 10 time slower than the CFLF composites on the same grid. The FCF 3D scheme is about 2 times faster than

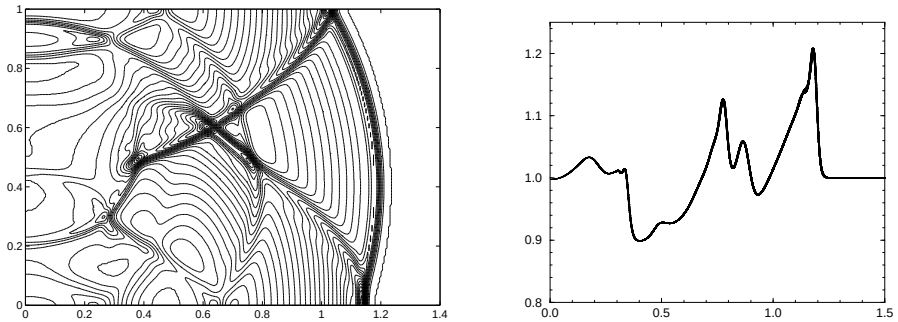

(a) (b)

FIGURE 4. (a) Contour plot of pressure at the $y = 0$ face, (b) Scatter plot of pressure versus the distance from the z axis at the plane $z = 0.4$.

the CF scheme. For the smooth radial 3D problem from [15, 16] the FCF scheme is about 15 times faster than the CLAWPACK [15, 16] code on the same grid, however, CLAWPACK produces more accurate results.

The composite schemes also work well on trapezoidal meshes [8] and probably can be generalized to other types of grids.

To conclude we do not claim that the composite schemes are the best ones, however they are simple, fast, work remarkably well for many problems and can provide a very simple way to get a feeling for the solution of a problem before investing a lot of time in developing a more elaborate method.

Acknowledgement

Both authors were partially supported by the CHAMMP program of the US Department of Energy. R. Liska was supported in part by the National Science Foundation grant CCR-9531828 , by the Ministry of Education of Czech Republic program Kontakt (Project ME 050 (1997)), his participation in the conference was supported by the Ministry of Education of Czech Republic (Project PG 98214) and by ETH Zürich and would like to thank the Institute for Geophysics and Planetary Physics of the Los Alamos National Laboratory for hosting his visit at Los Alamos.

References

[1] D. D. Houghton and A. Kasahara. Nonlinear shallow fluid flow over an isolated ridge. *Comm. Pure Appl. Math.*, 21:1–23, 1968.

[2] R. Liska and B. Wendroff. Composite schemes for conservation laws. *SIAM J. Numer. Anal.*, 1998. to appear, Technical Report LA-UR 96-3589, LANL, Los Alamos, 1996.

[3] R. Liska and B. Wendroff. Analysis and computation with stratified fluid models. *J. Comp. Phys.*, 137:212–244, 1997.

[4] H. Nessyahu and E. Tadmor. Non-oscillatory central differencing for hyperbolic conservation laws. *J. Comp. Phys.*, 87(2):408–463, 1990.

[5] G.S. Jiang, D. Levy, C.T. Lin, S. Osher, and E. Tadmor. High-resolution non-oscillatory central schemes with non-staggered grids for hyperbolic conservation laws. *SIAM Journal on Numerical Analysis*, 1997. in press.

[6] X.D. Liu and S. Osher. Convex eno high order multi-dimensional schemes without field by field decomposition or staggered grids. *J. Comp. Phys.*, 1997. submitted.

[7] T. Boukadida and A.-Y. LeRoux. A new version of the two-dimensional Lax-Friedrichs scheme. *Math. Comp.*, 63:541–553, 1994.

[8] R. Liska and B. Wendroff. 2d shallow water equations by composite schemes. Technical Report LAUR-97-4879, LANL, Los Alamos, 1997. submitted to Int. J. for Numerical Methods in Fluids.

[9] C. W. Schulz-Rinne, J. P. Collins, and H. M. Glaz. Numerical solution of the Riemann problem for two-dimensional gas dynamics. *SIAM J. Sci. Comput.*, 14:1394–1414, 1993.

[10] P. D. Lax and X.-D. Liu. Solution of two dimensional Riemann problem of gas dynamics by positive schemes. *SIAM J. on Scientific Comp.*, 19(2):319–340, 1998.

[11] Guan-Shan Jiang and Chi-Wang Shu. Efficient implementation of weighted eno schemes. *J. Comp. Phys.*, 126:202–228, 1996.

[12] H. Hong, R. Liska, and S. Steinberg. Testing stability by quantifier elimination. *J. Symbolic Computation*, 24(2):161–187, 1997. Special issue on Applications of Quantifier Elimination.

[13] B. Eilon, D. Gottlieb, and G. Zwas. Numerical stabilizers and computing time for second order accurate schemes. *J. Comp. Phys.*, 9:387–397, 1972.

[14] W. F. Noh. Errors for calculations of strong shocks using an artificial viscosity and artificial heat flux. *J. Comp. Phys.*, 72:78–120, 1987.

[15] J.O. Langseth and R.J. LeVeque. Three-dimensional euler computations using clawpack,. In P. Arminjon, editor, *Conf. on Numer. Meth. for Euler and Navier-Stokes Equations*, Montreal, 1995. to appear.

[16] J.O. Langseth and R.J. LeVeque. A wave propagation method for three-dimansional hyperbolic conservation laws. Technical report, University of Washington, Seatle, WA, 1997.

[1]Faculty of Nuclear Sciences and Physical Engineering
Czech Technical University in Prague
Břehová 7, 115 19 Prague 1, Czech Republic
[2]Group T-7, Los Alamos National Laboratory
Los Alamos, NM 87544, USA
E-mail address: liska@siduri.fjfi.cvut.cz,bbw@lanl.gov